⊙ 研究論文

Turbulent Flow and Heat Transfer in Concentric Annuli Depending on Position of Wall Roughness

AHN, Soo Whan · SON, You Sik

벽면거칠기위치에 따른 이중동심관내의 난류유동과 열전달

안 수 환* · 손 유 식*

Key words : Turbulent Fluid Flow(난류유동), Heat Transfer(열전달), Rough Annuli(거친이중관), Heat Transfer Ratio(열전달율)

Abstract

직경 비가 0.56인 이중동심관에 내외측모두 매끈한 벽면, 벽면 거칠기를 안측, 외측, 그리고 양측 모두의 4경우에 대한 난류 유동과 열전달특성을 실험과 이론으로 연구하였다. 시간평균속도분포, 마찰계수, 그리고 최대 속도 지점과 전단응력이 0인 지점들을 피토튜브와 X형 열선 풍속계로 측정하였다. 이중동심관내에서 4가지경우에 따른 사각돌출형 거칠기효과가 난류 유동과 열전달에 미치는 영향을 수정난류모델을 기초로 하여 연구하였다. 직경비, 거칠기 위치, 레이놀즈수, 그리고 프란틀수 등의 여러변수에의해서 난류 유동과 열전달을 고찰하였다. 본 연구는 전체적 효율 측면에서 유리하게 열전달율을 향상시킬 수 있는 거칠기 구조를 밝혔다.

NOMENCLATURE

a	thermal diffusivity
c	specific heat
e	roughness height
K	mixing length constant
De	equivalent diameter
P	pitch between tips of roughness elements
Pr_t	turbulent Prandtl number
q	heat flux
R_o	the location of zero shear stress
R_1	inner tube radius
R_2	outer tube radius
R_j^+	$R_j(\tau_{R2}/\rho)0.5/\nu$
S	$R_2 - R_1$
T_j^+	$(T_{R1} - T_j)C\tau_{R2}/[q_{R2}(\tau_{R2}/\rho)^{0.5}]$
u_j^+	$u_j/(\tau_{R2}/\rho)^{0.5}$
y_j^+	$y_j(\tau_{R2}/\pi)^{0.5}/\nu$
Z_{Rj}	imaginary location where $u_j=0$
α	radius ratio, R_1/R_2

* 경상대학교 기관공학과 (원고접수일 : 96년 9월 7일)

δ_j $|R_m - R_{1,2}|$
Δ δ_j^+/R_j^+
ε eddy diffusivity
e roughness height
ζ_j y_j^+/δ_j^+
$\overline{\tau_{R1,2}}$ averaged values of core and outer wall shear stresses

Subscripts :

H Heat
i inner region from zero shear stress position
j i or o
M momentum
o outer region from zero shear stress position
R radius
r rough
s smooth
sub sublayer boundary
t turbulent

1. INTRODUCTION

Short of a complete theory of turbulent flow, needed knowledge of the fully developed turbulent flow in an annular pipes, involves information on friction factors, velocity distributions, the turbulence structure and heat transfer. Such knowledge is available for the two other cases in which fully developed flow is one - dimensional ; i. e., flow in circular pipes and flow between parallel planes. However, complete information has not been available for flow in annular pipes.

For this reason, it has attracted the attention of researchers in the hope that its analysis would elucidate some of the evident difference between these two basic flow situations. However, they have investigated the turbulent flow and heat transfer in smooth annuli ; while not much studies have reported[1,2,3,4] on the turbulent flow and heat transfer in rough annuli. In heat exchangers with enhanced heat transfer surfaces which are sufficiently rough will have increased heat transfer coefficients because the turbulence setup in the wake of each roughness element will penetrate into the laminar sublayer. For the completely rough region in duct follow with relatively coarse and tightly spaced roughness elements, the friction factor is shown to be independent of the Reynolds number. Since the roughness of the surface not only increases the heat transfer rate, but also produces additional pressure losses, the heat transfer per unit pumping power expended may not be improved.

In present study, the resultant effect of artificial roughness is determined from a comparison of results of rough and smooth annuli in terms of a modified turbulence model. Accordingly, the desirable artificial roughness structure in annuli has obtained.

2. ANALYTICAL STUDY

2.1 Assumptions

The governing equations are broken into smooth and rough sides. For the analysis, we introduce the following assumptions :

1. The annuli is concentric. While the outer wall surface is insulated, the inner surface has constant heat flux.
2. Velocity and temperature fields in the annulus are fully developed.
3. The turbulent Prandtl number is taken unity.

2.2 Velocity and Temperature Distributions

The basic equations governing the transport of momentum can thus be written as :

$$\frac{\tau_j}{\rho}=(\nu+\varepsilon_M)_j\frac{\partial u_j}{\partial y_j} \quad (1)$$

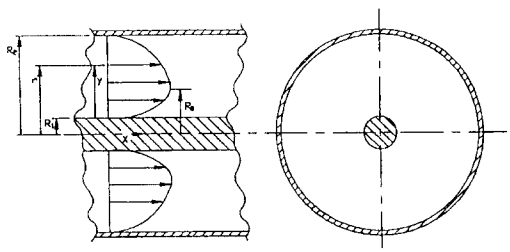

Case(a)

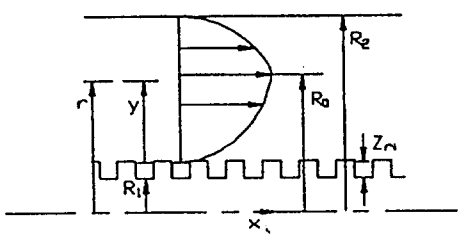

Case(b)

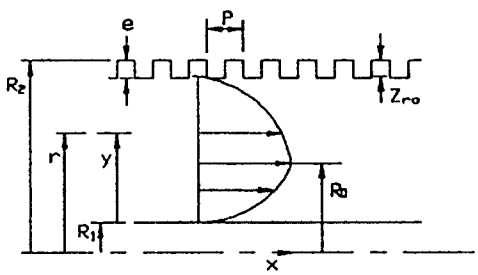

Case(c)

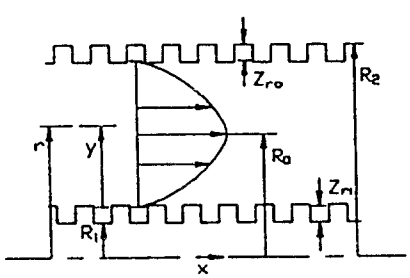

Case(d)

Fig. 1 Geometry of roughness element

$$-\frac{q}{c\rho}=(a+\varepsilon_H)\frac{\partial T}{\partial r} \quad (2)$$

From Eqs. (1) and (2), the temperature gradient can be obtained as Eq. (3) in nondimensional parameters

$$\frac{\partial T_j^+}{\partial \zeta}=\pm\frac{\partial u_j^+}{\partial \zeta}\left(\frac{1+\varepsilon_M/\nu}{1/Pr+1/Pr_t\varepsilon_M/\nu}\right)_j\frac{q_j/q_{R1}}{\tau_j/\tau_{R2}} \quad (3)$$

where +ve is for j=i and −ve for j=o. From a force balance made on the element, the shear stress distributions(τ_j/τ_{R2}) are obtained from force balance. And since the heat condition is a constant heat flux at the core tube only, the heat flux distributions(q_j/q_{R1}) are obtained from an energy balance made on the element,

2.3 Velocity Gradient

We can obtain the velocity gradient from Eq. (1) for the smooth wall ; that is, the whole region of case (a), the outer region from zero shear stress position of case (b) and the inner region from zero shear stress position of case (c) as follows

$$\frac{\partial u_i^+}{\partial \zeta_i}=\delta_i^+\frac{\tau_i/\tau_{R1}}{1+(\varepsilon_M/\nu)_i}\frac{\tau_{R1}}{\tau_{R2}} \quad (0\le\zeta_i\le 1) \quad (4)$$

$$\frac{\partial u_o^+}{\partial \zeta_o}=\delta_o^+\left[\frac{\tau_o/\tau_{R2}}{1+(\varepsilon_M/\nu)_o}\right] \quad (0\le\zeta_o\le 1) \quad (5)$$

And considering the rough wall ; that is, the outer region from zero shear stress position at the case (c), the inner region from zero shear stress position at the cases (b) and and the whole region at the case (d), we obtain the following velocity gradients

$$\frac{\partial u_i^+}{\partial \zeta_i}=\frac{u_{\tau_{R1}}}{u_{\tau_{R2}}}\frac{1}{k_i\zeta_i}\left(\frac{Z_{ri}^+}{\delta_i^+}\le\zeta_i\le 1\right) \quad (6)$$

$$\frac{\partial u_o^+}{\partial \zeta_o}=\frac{1}{k_o\zeta_o}\left(\frac{Z_{ro}^+}{\delta_o^+}\le\zeta_o\le 1\right) \quad (7)$$

2.4 Eddy Diffusivity for Momentum, ε_M

For the smooth wall, the models originally due to van Driest[5] and Reichardt[6] were modified to suit to the present flow channel geometry as

$$(\varepsilon_M/\nu)_{it} = (k_i\delta_i^+/6)[1-(1-y_i^+/\delta_i^+)^2]\,x[1+2(1-y_i^+/\delta_i^+)^2]\frac{u_{\tau R1}}{u_{\tau R2}} \quad (y_{isub}^+ \le y_i^+ \le \delta_i^+) \tag{8}$$

$$(\varepsilon_M/\nu)_{ot} = (k_o\delta_o^-/6)[1-(1-y_o^+/\delta_o^-)^2]\,x[1+2(1-y_o^+/\delta_o^+)^2] \quad (y_{osub}^+ \le y_o^- \le \delta_o^+) \tag{9}$$

$$(\varepsilon_M/\nu)_{jsub} = k_j^2 y_j^{+2}[1-\exp(-y_j^+/A_j^+)]^2\left|\frac{\partial u_j^+}{\partial y_j^+}\right| \quad (0 \le y_j^+ \le y_{jsub}^+) \tag{10}$$

For the rough region, we use the Prandtl mixing length theory to be obtained as

$$(\varepsilon_M/\nu)_j = k_j^2 y_j^{+2}\,|\,\partial u_j^+/\partial y_j^-\,| \quad (Z_{rj}^+ \le y_i^+ \le \delta_i^+) \tag{11}$$

2.5 Reynolds Number, Friction Factor and Nusselt Number

2.5.1 Reynolds number

$$Re = \frac{2u_b(R_2-R_1)}{\nu} = 2u_b^+(R_2^+-R_1^+) \tag{12}$$

2.5.2 Friction factor

$$f = \frac{\overline{\tau_{R1,2}}}{0.5\rho u_b^2} \tag{13}$$

2.5.3 Nusselt number

$$Nu = 2(R_2-R_1)h/K = \frac{2(R_2^+-R_1^+)Pr}{T_b^+} \tag{14}$$

where the heat transfer coefficient, h, is $q_{R1}/(T_{R1}-T_b)$. The bulk temperature (T_b) can be defined in dimensionless parameters as :

For Case(a)

$$T_b^+ = \frac{4}{Re(1+\alpha)}[\alpha\delta_i^+\int_0^1(1+\Delta_i\zeta_i)u_i^+T_i^+d\zeta_i + \delta_o^+\int_0^1(1-\Delta_o\zeta_o)u_o^+T_o^+d\zeta_o] \tag{15}$$

For Case(b)

$$T_b^+ = \frac{4}{1+\alpha}\frac{1}{Re}[\alpha\delta_i^+\int_{\frac{Z_{ri}^+}{\delta_i^+}}^1(1+\Delta_i\zeta_i)u_i^+T_i^+d\zeta_i + \delta_o^+\int_0^1(1-\Delta_o\zeta_o)u_o^+T_o^+d\zeta_o] \tag{16}$$

For Case(c)

$$T_b^+ = \frac{4}{1+\alpha}\frac{1}{Re}[\alpha\delta_i^+\int_0^1(1+\Delta_i\zeta_i)u_i^+T_i^+d\zeta_i + \delta_o^+\int_{\frac{Z_{ro}^-}{\delta_o^+}}^1(1-\Delta_o\zeta_o)u_o^+T_o^+d\zeta_o] \tag{17}$$

For Case(d)

$$T_b^+ = \frac{4}{Re(1+\alpha)}[\alpha\delta_i^+\int_{\frac{Z_{ri}^+}{\delta_i^+}}^1(1+\Delta_i\zeta_i)u_i^+T_i^+d\zeta_i + \frac{1}{\alpha}\delta_o^+\int_{\frac{Z_{ro}^+}{\delta_o^+}}^1(1-\Delta_o\zeta_o)u_o^+T_o^+d\zeta_o] \tag{18}$$

3. EXPERIMENTAL STUDY

The experimental programme undertaken the present study is designed to check out velocity profiles, friction factor, and turbulent shear stresses for radius ratio of 0.56 at P/e=2. The working fluid is chosen as air in atmospheric conditions due to purposes of economical construction of test facilities and also availability of information on physical properties. The static pressure measurements are made with a MKS pressure transducer and the calibration of which is checked against a micro-manometer(FCO-12) at frequent intervals. The total dimension of the main apparatus is about 6.1 meter in length. Air is drawn through a flow measuring orifice into an air filter and then through a bell-mouthed contraction section into the test section by a blower(0.8kW, 3400RPM) located at the extreme downstream end. The annular test section consists of core tubes having three different outer diameters and outer tubes having 97mm inner diameter as in Table 1. A specially designed traversing mechanism carries the measuring instrument.

Table 1 Essential dimensions unit : mm

	tube	O. D.	I. D	material	$\alpha = R_1/R_2$	$De = 2R_2 - 2R_1$
Case(a)	outer	113	97	copper	0.56	43
	core	54	52	copper		
Case(b)	outer	113	97	copper		
	core	54	51	acryl		
Case(c)	outer	117	97	Al - alloy		
	core	54	52	copper		
Case(d)	outer	117	97	Al - alloy		
	core	54	51	acryl		

With this mechanism, the relative radial displacement of a probe is measured within 0.025 mm by electrical contact. The core tubes are supported at three locations by 3 - point carriers which allow for radial adjustments of the core tube. When the test sections were assembled and aligned, the concentricity of the core to the outer tube was checked. Two constant temperature anemometers (C. T. A., TSI Model 1054A) with an X - type hotwire probe and a universal waveform analyzer(D - 6000 Model 611, Data Precision Inc.) are used and the calibration is done with the Pitot tube of 4 mm in diameter and 350mm in length and digital micro - manometer(Model FCO - 12). The outputs from C.T.A. Bridge that are prevented from aliazing by passing through 5 kHz low - pass filter are simultaneously sampled as digital values by means of 14 - bit A/D converter equiped in the universal waveform analyzer, and then are recorded at the diskettes through Data Recorder, with a sampling rate of 10,000 units per second corresponding to Niquist sample period. All the measurements are carried out only late in the night to avoid disturbances on the main power supply. The range of Reynolds number covered is from 15,000 to 66,000 approximately. The pressure and temperature of the ambient are also recorded before each run.

4. RESULTS AND DISCUSSION

An example of predicted velocity profiles is compared with the experimental measurement in Fig. 2. The fairly lower velocity in the vicinity of the rough outer wall seems to be attributed to the pressure induced by the radial flow components. The velocity profiles obtained from Eq. (4) to (7) agree reasonably well with the experimental data. And Park's results[7] are slightly different from present studies because those are measured with a Pitot tube.

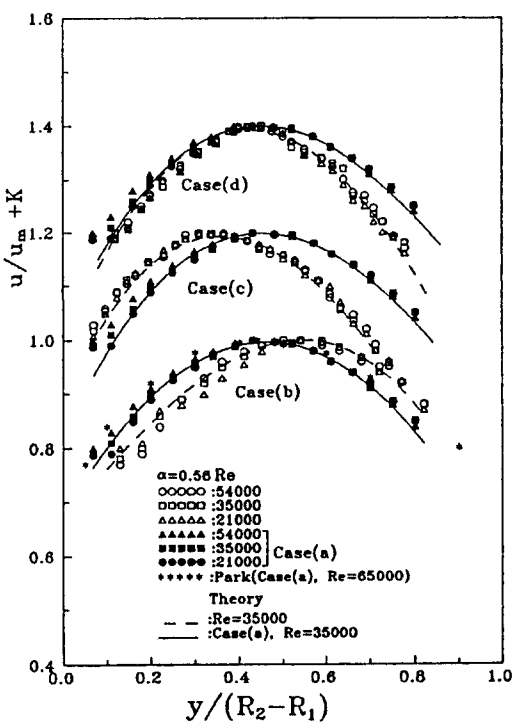

Fig. 2 Velocity distribution

Fig. 3 shows the variations of maximum velocity and zero shear stress positions in Case(b) depending on Reynolds number, at which the maximum velocity positions are located closer to the core tube. This is because

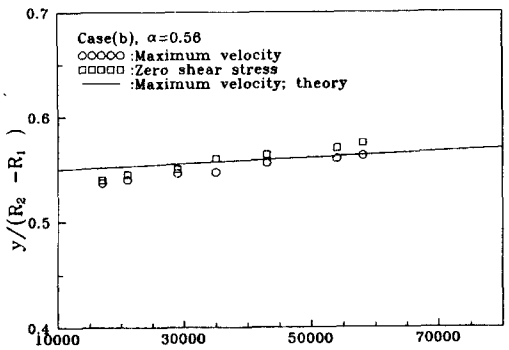

Fig. 3 Example of maximum velocity against zero shear stress position

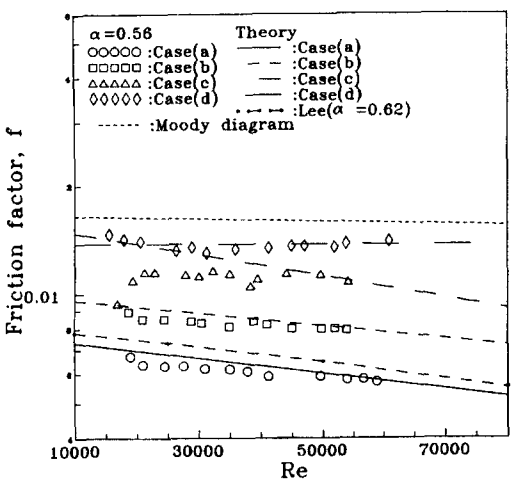

Fig. 4 Friction factor

the velocity profiles become more insensitive to the wall roughness than the shear stress distributions. Maximum velocity positions are in a reasonable line with the theoretical results. The friction factors obtained from zero shear stress positions in Fig. 3 and the static pressure drops have been shown in Fig. 4, at which the friction factor is largest at Case (d), this tendency is probably attributed to the highest increase in the pressure drop. For the comparison at Case(a), Lee's theoretical results are included. There is a little deviation between Lee's and present studies. It is supposed to be

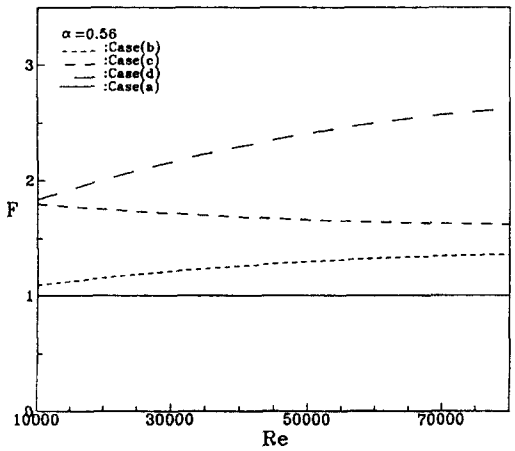

Fig. 5 Roughness position on friction factor ratio, F

from difference of radius ratio(α). And the figure has shown that the predicted friction factors by Moody diagram are unavailable for annular pipes. In Fig. 5, the increase in friction factor due to the roughness elements is normalized by that of the Case (a). The normalized friction factor is defined as :

$$F = f_r / f_s \tag{19}$$

F is highest at Case (d) for the range of the parameters studied. This tendency can be explained from the fact that the friction factor is strongly subjected to the roughness elements. Heat transfer in terms of Nu is also normalized as :

$$H = Nu_r / Nu_s \tag{20}$$

The effects of roughness position and Pr on H can be depicted in Fig. 6 and the trends are similar to those observed in Fig. 5. The resultant effect of artificial roughness is determined from a comparison of results of rough and smooth surfaces by virtue of the heat transfer increase relative to the increase in pressure losses. This may be expressed in terms of a non - dimensional parameter, H/F, which is defined as :

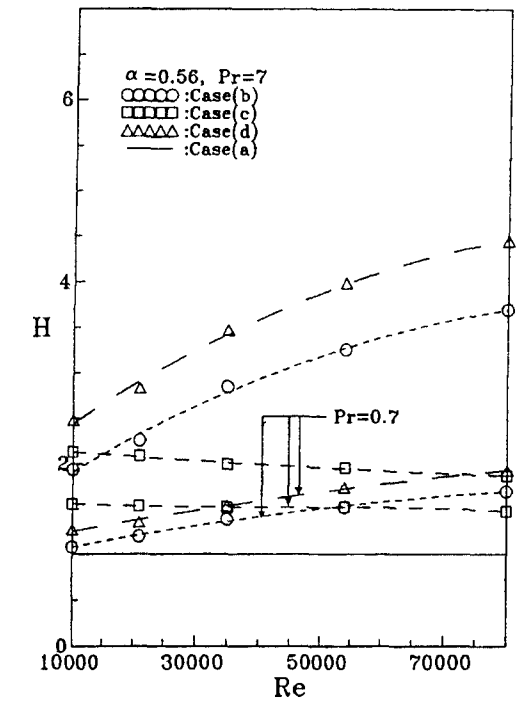

Fig. 6 Roughness position on heat transfer ratio, H

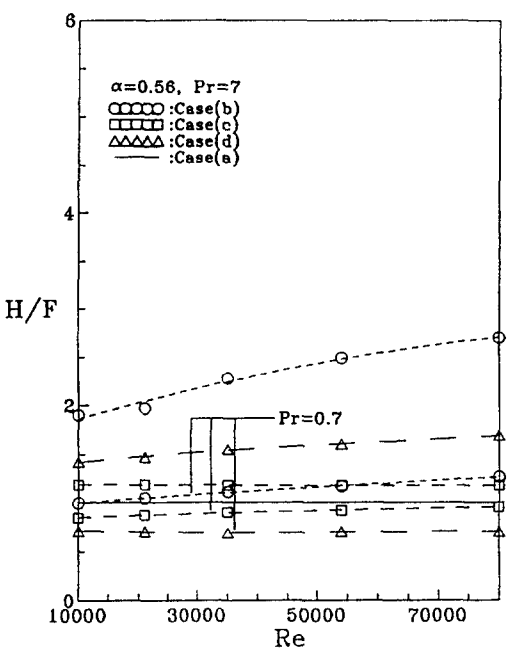

Fig. 7 Effects of Re and roughness position on H/F

$$H/F=(Nu_r/Nu_s)/(f_r/f_s) \quad (21)$$

H/F > 1 suggests that the increase in heat transfer due to roughness is greater than the increase in pressure loss due to roughness and therefore it is advantageous to have the particular roughness elements from the overall efficiency point of view. Fig. 7 shows the effects of Reynolds number and position of roughness element. The ratio of H/F increases with increasing Pr at the case of Pr=0.7, and is higher in annuli with the rough core tube rather than with the rough outer tube because we assume in the analysis that the core tube is heated as constant heat flux, while the outer tube is insulated.

5. CONCLUSIONS

From the analytical and experimental investigation, we can derive the conclusion that the effects of roughness position, radius ratio(α), relative roughness height, Reynolds and Prandtl numbers on the ratio H/F were identified for a turbulent flow induced by square-ribbed surface roughness elements. The study demonstrates that 1) certain artificial roughness elements can be used to enhance heat transfer rates with advantages from the overall efficiency point of view, 2) the design for Case (b) is something advantageous over for Cases (c) and (d) at Pr=0.7 and 3) it is more advantageous at higher Prandtl number.

ACKNOWLEDGEMENT

This paper was supported in part by NON DIRECTED RESEARCH FUND, Korea Research Foundation, 1995.

REFERENCE

1) Durst, F., On Turbulent Flow through Annular

Passages with Smooth and Rough Core, M. Sc. Thesis, Imperial College, (1968).

2) Kim, K. C., Ahn, S. W. and Lee, B. G., Turbulence Structure of Flow in Concentric Annuli with Rough Outer Wall, J. of KSME, 18 - 9, (1994 - 9), 2443 - 2453.

3) Lee, Y. P., Ahn, S. W. and Y. Lee, Turbulent Fluid Flow and Heat Transfer Induced by Square - Ribbed Surface Roughness in Concentric Annuli, Ninth International Heat Transfer Conference, (1990), 4 - MC - 20, Jerusalem,.

4) Lee, Y. P., Ahn, S. W. and Lee, Y., Enhanced Turbulent Heat Transfer Induced by Square - Ribbed Wall Roughness in Concentric Annuli, Proc. of The Second KSME - JSME Fluids Engineering Conference, Seoul, (1990 - 11), 2, 293 - 298.

5) van Driest, E. R., On Turbulent Flow Near a Wall, J. of Aero. Sci., (1956), 23, 485.

6) Reichardt, H., Vollstandige Darstellung der turbulenten Geschwindigekeitsverterilung in glatten Leitungen, Z. amgew. Mathematic und Mechanik, (1951), 31, 208 - 219.

7) Park, S. D., Developing Turbulent Flow in Concentric Annuli : An Analytical and Experimental Study, (1971), Ph. D. Thesis, Dept. of Mech. Eng., University of Ottawa.